JOURNAL OF DEGRADED AND MINING LANDS MANAGEMENT
Volume 10, Number 4 (July 2023):4629-4645, doi:10.15243/jdmlm.2023.104.4629
ISSN: 2339-076X (p); 2502-2458 (e), www.jdmlm.ub.ac.id

Research Article

The prediction of land use and land cover change and its impact on soil erosion and sedimentation in the Musi Hydropower-Plant catchment area in Bengkulu Province

Sukisno[1,2], Widiatmaka[3*], Moh. Yanuar Jarwadi Purwanto[4], Bambang Pramudya Noorachmat[5], Khursatul Munibah[6]

[1] Graduate Study Program of Natural Resources and Environmental Management, IPB University, Bogor, West Java, Indonesia
[2] Department of Agriculture Cultivation, Faculty of Agriculture, University of Bengkulu, Bengkulu, Indonesia
[3] Department of Soil Science and Land Resources, IPB University, Bogor, West Java, Indonesia
[4] Department of Civil and Environment, IPB University, Bogor, West Java, Indonesia
[5] Department of Agricultural and Bio-system Engineering IPB University, Bogor, West Java, Indonesia
[6] Department of Soil Science and Land Resources, IPB University, Bogor, West Java, Indonesia

[*]corresponding author: widiatmaka@ipb.ac.id; widi.widiatmaka@yahoo.com

Article history:
Received 16 December 2022
Accepted 13 February 2023
Published 1 July 2023

Keywords:
LULCC
Musi Hulu
sediment yield
soil erosion

Abstract

The Musi Hydropower-Plant catchment area is susceptible to soil erosion and sedimentation. Therefore, this research aimed to predict land use and land cover changes (LULCC) as well as their impact on soil erosion and sedimentation in the Musi Hydropower-Plant catchment area. The prediction of LULCC was calculated using Land Change Modeler module on IDRISI Terrset, while soil erosion and sedimentation were estimated with the Revised Universal Soil Loss Equation (RUSLE) and Sediment Delivery Ratio (SDR) models. The result showed that forest cover and paddy fields decreased significantly from 18,580 ha and 4,044 ha to 12,907 ha and 2,019 ha, respectively, in the periods of 1993 to 2019 and were predicted to reduce until 2032. Meanwhile, the built-up area and dry agricultural land increased from 818 ha and 2,116 ha in 1993 to 2,229 ha and 5,778 ha in 2019, which is expected to increase until 2032. The estimation of soil erosion rate also gave an increase from 75 t/ha/year to 113 t/ha/year, continuing to reach 122 t/ha/year until 2032. The escalation of soil erosion rate contributed to the change of sediment yield from 68.048 t/year in 1993 to 103.190 t/year in 2019, which is estimated to reach 111.028 t/year. These results are expected to be used by decision-makers and policymakers for the operation of the Musi Hydropower-Plant and the catchment area maintenance.

To cite this article: Sukisno, Widiatmaka, Purwanto, M.Y.J., Noorachmat, B.P. and Munibah, K. 2023. The prediction of land use and land cover change and its impacts on soil erosion and sedimentation in the Musi Hydropower-Plant catchment area in Bengkulu Province. Journal of Degraded and Mining Lands Management 10(4):4629-4645, doi:10.15243/jdmlm.2023.104.4629.

Introduction

Land use and land cover (LULC) are essential elements for interpreting and monitoring the earth's surface phenomenon (Kokla et al., 2015). The land is the place where all human activities are being performed and the origins of goods for these operations (Briassoulis, 2020). According to Comber et al. (2015), land cover describes observable features on the earth's surface, such as soil, water, and vegetation, while land use emphasizes the intentions explaining land cover, including the changes made by

anthropogenic activities. Meanwhile, the dynamic process of interaction between LULC can be represented by human activities, namely agriculture intensification and urbanization, or natural actions such as floods and landslides (Chaves et al., 2020). LULCC can be used to evaluate land resources degradation (Mujiyo et al., 2021), its impact on water yield and runoff (Wang et al., 2018), soil erosion (Obiahu and Elias, 2020; Millazo et al., 2022) and sedimentation (Gwapedza et al., 2021). The sub-watershed of Musi Hulu is upstream of the Musi River, located in Bengkulu Province, Indonesia. As the catchment area of Musi Hydropower-Plant, the sub-watershed is susceptible to land degradation. The presence of LULCC (Sukisno et al., 2021) altered the soil erosion and sedimentation, ensuing a disturbance in the reservoir function (Amri et al., 2014).

Soil erosion and sedimentation are detrimental impacts of LULCC. The conversion of forest cover to agricultural land results in increasingly eroded soil. The easily eroded soil contributed to the high potential of soil loss and increasing sedimentation. Kidane et al. (2019) informed that the dynamic of LULCC contributed to the increasing soil erosion and sedimentation in Ethiopia. Yan et al. (2018) described that soil erosion in Loss Plateau, China, decreased in the order of residential area, farmland, grassland, and forest. Meanwhile, Muddarisna et al. (2021) stated that the leaves and roots of vegetation are the most important part in controlling soil loss. The increasing soil erosion and sedimentation rates influenced the functionality and lifetime of reservoirs (Atulley et al., 2022; Patro et al., 2022). Generally, LULCC were difficult to access, time-consuming and expensive. The growth of remote sensing and geographical information system has provided the tools and methodology for LULCC analysis. LULCC are easy to analyze and simpler and more reliable (Dangulla et al., 2020). Integration of these technologies is also very helpful in the analysis of the impact of LULCC on soil erosion and sedimentation (Ejegu and Yegizaw, 2021; Endalew and Biru, 2022; Jothimani et al., 2022).

This study aimed to predict land use and land cover change and its impact on soil erosion and sedimentation in the Musi Hydropower-Plant catchment area. This study was carried out to (1) classify land use and land cover in 1993, 2006, and 2019, (2) predict land use land cover change in 2032, and (3) estimate soil erosion and sedimentation rate in 1993, 2006, 2019, and 2032.

Materials and Methods

Research location

The Musi Hydropower-Plant catchment area is positioned within 102°22'18.98" to 102°38'38.93" East Longitude and 3°6'28.873" to 3°33'57.44" South Latitude and located on the south part of Sumatera Island as shown in Figure 1. The catchment area extended into five districts, Rejang Lebong, Kepahiang, Center of Bengkulu, North of Bengkulu and Lebong Regency, Bengkulu Province, Indonesia, with a total area 60,616.4 ha. The Musi River flows from the upland area to the main river and ends on the east coast of Sumatera Island. However, the establishment of the power plant in 2006 modified the flow. After flowing from the catchment area to the reservoir, most of the water used to generate the power plant spill out to Lemau River and ends up on the west coast of Sumatera Island, as shown in Figure 1. The average rainfall in the area is very high, with an annual value of more than 2,500 mm/year. The highly monthly rainfall is recorded in December, while July has the lowest. Rainfall data were collected from the Meteorological, Climatological, and Geophysical Agency of Pulau Baai Bengkulu, Indonesia.

The elevation of the area spread out from 500 to 2,500 masl. The area is dominated by land with elevation 500-1,000 masl (62%), followed by 1,000-1,500 masl (30.42%), 1.500 masl (5.5%) and >2.000 masl (1.14%). Most of the area is dominated by land with a slope of 25-45% (30.34%), followed by 15-25% (22.32%), 8-15% (18.19%), 0-8% (16.47%), and >45% (12.67%). The elevation and slope data are derived from DEM that can be downloaded from http://tanahair.indonesia.go.id.

LULC change analysis

Satellite image taken by Landsat-5 (1993 and 2006) and Landsat-8 (2019) was classified into eight types of land use and land cover, namely built-up area, forest cover, water bodies, paddy fields, dry land agriculture, mixed dry land agriculture, bare soil/bare ground, and dry shrub. The satellite image was downloaded from www.earthexplorer.usgs.gov. Land use and land cover type are classified with the supervised classification (Ma et al., 2017) method in Arcgis 10.8.2. The accuracy classification was validated by verifying a fixed number of locations on the map and identifying those areas on the fields.

The prediction of LULCC used Land Change Modeler (LCM) model on IDRISI Terrset. The LCM approach integrates the Multilayer-Perceptron (MLP) with the Markov-Chain Method to model land transition probabilities using historical land use and land cover data and other geospatial datasets (Dangula et al., 2020). Land change prediction in LCM is a stepwise process from change analysis, transition potential modeling, and change prediction. In this research, LULCC 1993-2006 was used to predict LULC 2019. The predicted LULC 2019 is validated with the classified LULC 2019. When the Kappa coefficient >80%, the prediction continued to LULC 2032. The potential drivers causing land use change, such as elevation, slope, population density, and distance to roads, rivers, as well as settlements, were analyzed with Cramer's V test. A Cramer's V 0.15 suggests that the explanation of the variable is good.

Prediction of soil erosion

Soil erosion is estimated with the general equation of the Revised Universal Soil Loss Equation, which is popularly applied in most studies (Borrelli et al., 2021; Pandey et al., 2021). The RUSLE estimates the soil loss by multiplication of five erosion factors, including rainfall erosivity index, soil erodibility index, slope-length steepness index, cover management, and supporting practice.

$$A = R \times K \times LS \times C \times P \quad (1)$$

A is annual mean soil loss (t/ha/year), R is the Rainfall factor, K is the Soil erodibility factor, LS is slope length and steepness index, C is the cover-management factor, and P is the support practice factor.

Rainfall has a crucial contribution to soil erosion and sedimentation processes.

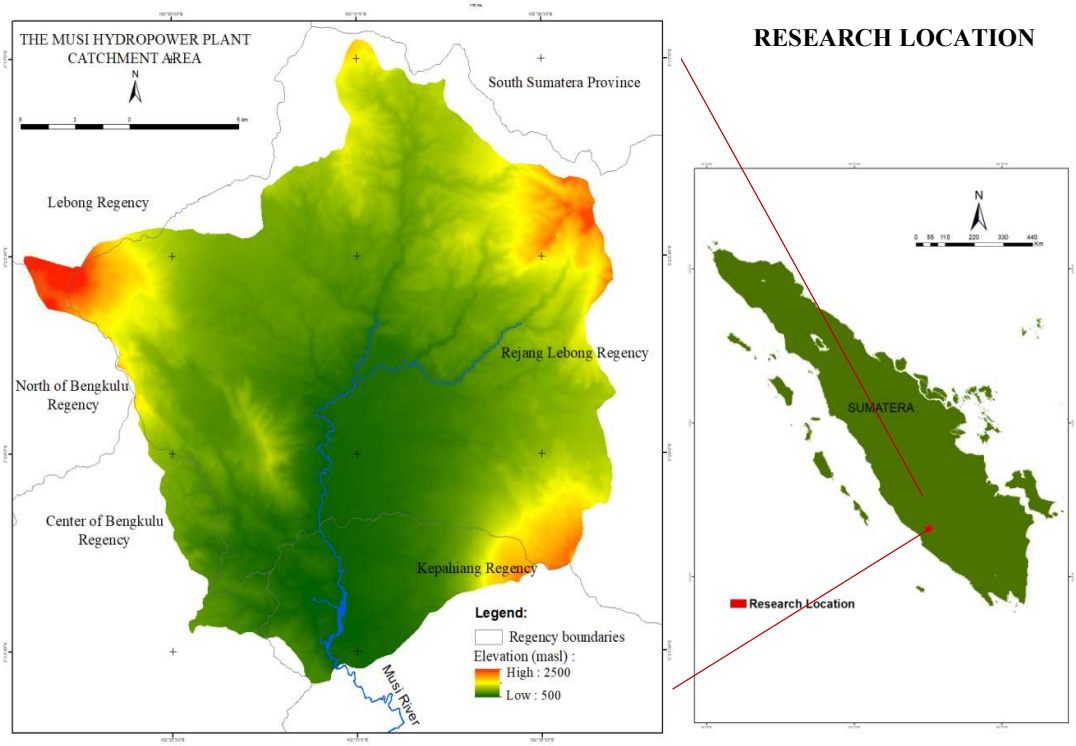

Figure 1. The study site Musi Hydropower-Plant catchment area.

Rainfall erosivity was determined using the Bols equation as follows:

$$R = \sum_{m=1}^{12}(Rm) \quad (2)$$

$$Rm = 6.119 \times (Rain)m^{1.21} \times (Days)m^{-0.47} \times (Max)m^{0.53} \quad (3)$$

R is rainfall erosivity, Rm is monthly rainfall erosivity, $(Rain)m^{1.21}$ is monthly rainfall, $(Days)m^{-0.47}$ is the number of rainy days, and $(Max)m^{0.53}$ is the maximum rainy day.

R in the catchment area shows varying values in 1993 from 1,768 MJmm/ha/year to 1,813 MJmm/ha/year. The R factor in 2006 and 2019 also varied from 1,927 MJmm/ha/year to 1,969 MJmm/ha/year and 1,950 MJmm/ha/year to 2,577 MJmm/ha/year. The R factors 1993, 2006, and 2019 are presented in Figures 2, 3, and 4.

Soil erodibility indicates the vulnerability of a soil type to disaggregate and transport within intense rainfall. The value range of K-factor is 0 to 1. The values close to 0 are the lowest vulnerable, the value range 0.2 to 0.4 is moderate, and values ≥0.4 are the majority vulnerable (Kulimushi et al., 2021). The equation of soil erodibility is:

$$K = \frac{2.173\, M^{1.14}\, (10^{-4})(12-1)+3.25(b-2)+2.5(c-3)}{100} \quad (4)$$

K is soil erodibility index, M is a result of function (% silt + % very fine sand) (100 - % clay), a is % soil organic matter, b is soil structure class, and *c* is soil permeability class.

The soil erodibility factor shows that the average of the K factor is 0.18, with minimum and maximum values of 0.04, and 0.36. The K factor is presented in Figure 5.

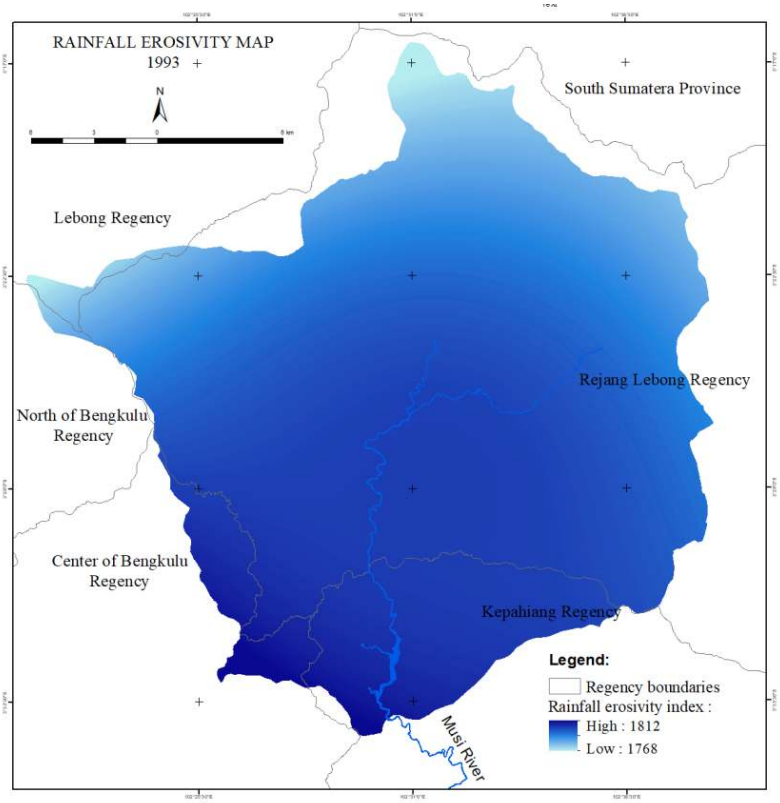

Figure 2. Map of R factor 1993.

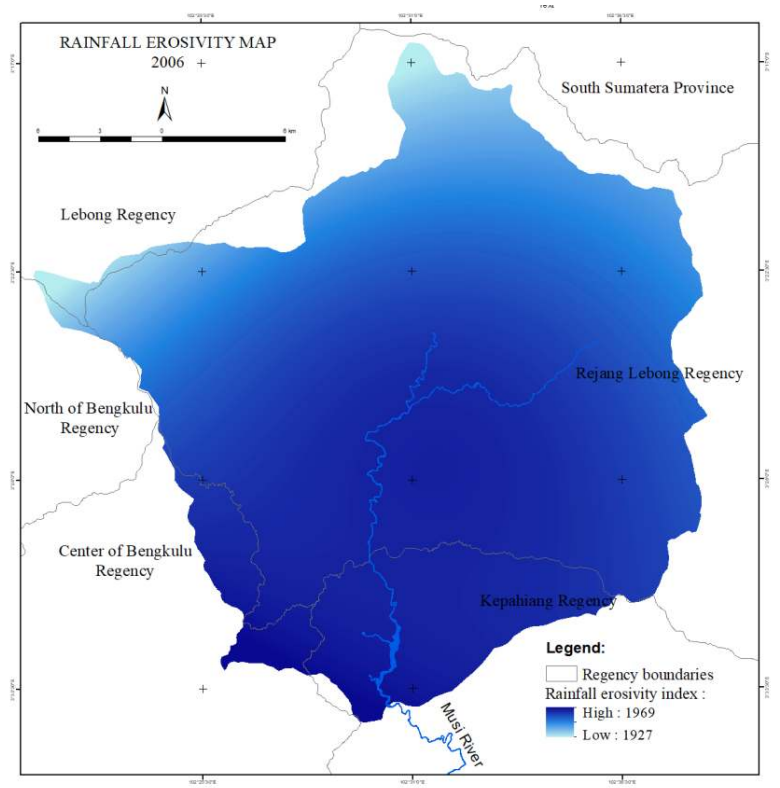

Figure 3. Map of R factor 2006.

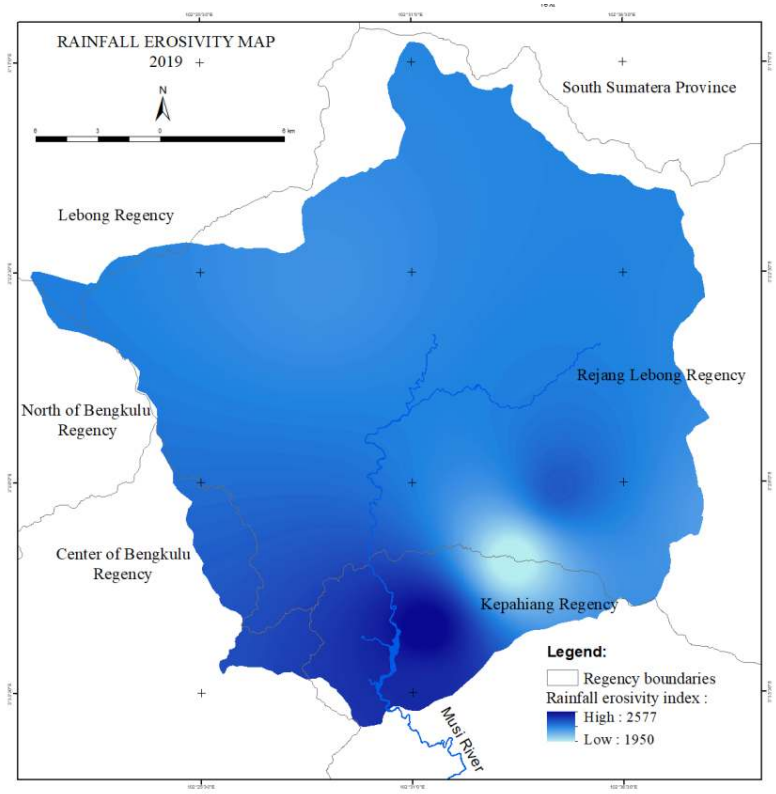

Figure 4. Map of R factor 2019.

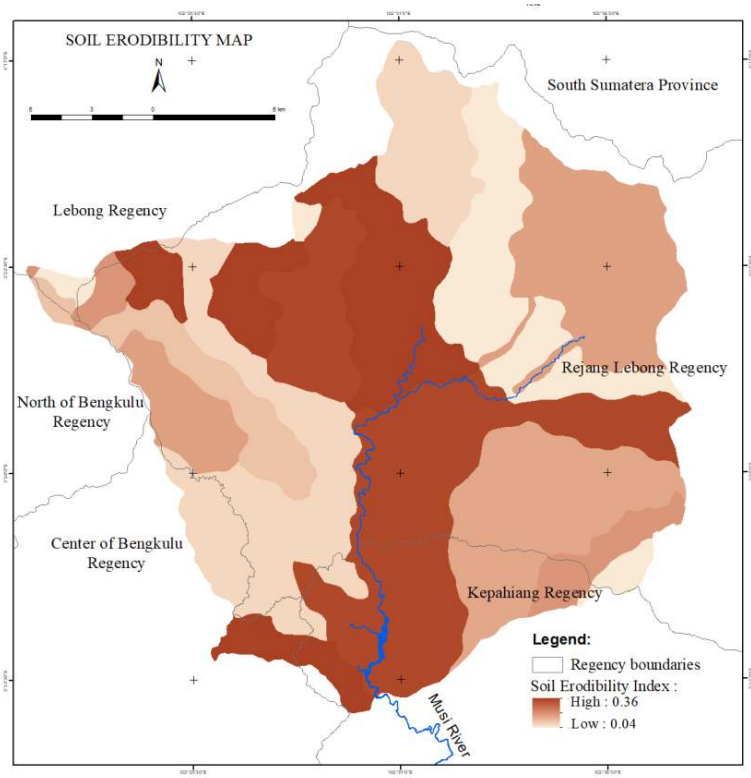

Figure 5. Map of K factor.

Topography has a significant impact on soil erosion. The slope-length steepness factor was estimated with the Wischmeier and Smith equation as follows:

$$LS = \left(\frac{X}{22.13}\right)^{m} (0.065 + 0.045\ S + 0.0065S^2) \quad (5)$$

LS is the slope-length steepness index. X is the cell resolution of the DEM. S is the slope, derived from the DEM. The variable m is the slope contingent variable, with the value varied from 0.2-0.5, subjected to the slope, which is 0.5 for ≥5%, 0.4 for slopes 3-5% and 0.3 for slopes 1-3%, and 0.2 for slopes <1.0%.

The average value of the slope-length steepness index is 0.41, with minimum and maximum values 0 and 29, as presented in Figure 6.

Vegetation cover is crucial in controlling soil erosion and sediment yields (Gwapedza et al., 2021). It can also be used to estimate soil erosion vulnerability in the past, present, and future. The value of the C-factor ranges from nearly 0-1 (Kulimushi et al., 2021). The value of C-factor in the catchment area varies from 0 to 1. The values of the C-factor are derived from land cover, as shown in Table 1.

The supporting practice factor describes the ratio of soil loss resulting from land with conservation practices such as contouring and terracing to the soil loss resulting from land with straight-row cultivation up and down the slope. It is the most important process to prevent and control soil erosion (Pandey et al., 2021).

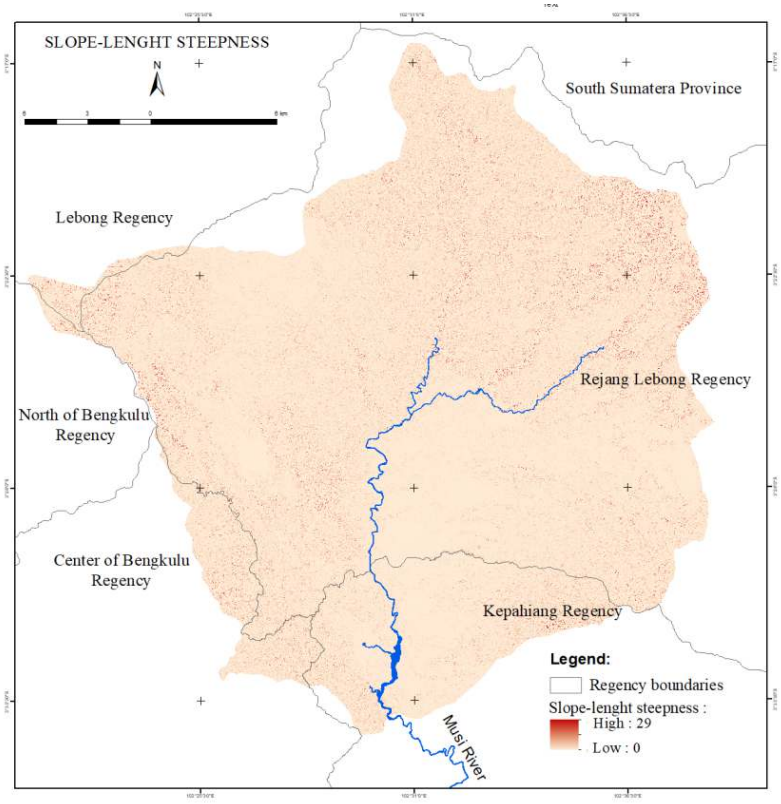

Figure 6. Map of slope-length steepness factor.

Table 1. Area coverage based on C-factor.

Land Use Type	C Value	Area (ha)		
		1993	2006	2019
Built-up area	0.15	818	1,412	1,412
Forest area	0.001	18,580	16,320	16,320
Water bodies	0	147	210	210
Paddy fields	0.01	4,044	3,023	3,023
Dry land agriculture	0.6	2,116	4,958	4,958
Mixed dry land agriculture	0.2	33,534	33,748	33,748
Bare soil/bare ground	1	487	383	383
Dry shrub	0.01	890	563	563
Total		60,616	60,616	60,616

The value of P-factor in the catchment area varies from 0-1, with an average value of 0.299 in 1993, 0.304 in 2006, 0.309 in 2019, and 0.312 in 2032. The vulnerability of soil erosion was reclassified into five severity groups, namely very light (0-15 t/ha/year), light (15-60 t/ha/year), medium (60-180 t/ha/year), heavy (180-480 t/ha/year), and very heavy (>480 t/ha/year). The prediction of the soil erosion rate in 2032 was based on the soil erosion factors with the assumption that except C-factor are stable (Millazo et al., 2022).

Sediment delivery ratio

The prediction of sediment rates was calculated based on the Sediment Delivery Ratio Model. The formula is:

$$SDR = 0.41A^{-0.3} \quad (6)$$

with SDR is the sediment delivery ratio, while A is the width of the catchment area (ha).

Results

Land use and land cover 1993-2019

The overall classification accuracy of the LULC was 96%, 91%, and 92% for 1993, 2006, and 2019 respectively. Since an accuracy of more than 85% is recommended, this indicates that the LULC map is acceptable. Similarly, the overall Kappa coefficient was 0.95, 0.89, and 0.91 for 1993, 2006, and 2019 respectively, as shown in Table 2. This indicated that the classified LULC map has a strong agreement with the ground reality (Foody, 2020). The LULC map of 1993, 2006, and 2019 are presented in Figures 7, 8 and 9.

Table 2. Classification accuracy assessment (%) of LULC 1993, 2006, and 2019.

Land Use Type	1993		2006		2019	
	UA	PA	UA	PA	UA	PA
Built-up area	100	94	95	95	95	95
Forest area	94	94	100	100	100	100
Water bodies	100	100	100	100	100	100
Paddy fields	93	100	90	82	82	90
Dry land agriculture	100	91	69	79	86	75
Mixed dry land agriculture	97	97	94	91	90	96
Bare soil/bare ground	100	100	100	89	89	89
Dry shrub	78	88	94	100	100	95
Overall accuracy	95.6		91.2		92.0	
Kappa coefficient	0.95		0.89		0.91	

UA= User accuracy; PA=Producer accuracy.

The annual land use type comparison shows the LULCC over time. The LULC in 1993 shows that mixed dry land agriculture dominated the area (55.3%), followed by forest cover (30.7%), paddy fields (6.7%), dry land agriculture (3.5%), dry shrub (1.5%), built-up area (1.3%), bare soil and water bodies (Table 3). The LULC in 2006 showed that mixed dry land agriculture and forest area still dominated the area, while dry land agriculture exceeded the paddy fields. The built-up area increases significantly, from 818 ha to 1,412 ha (Table 3). The area of mixed dry land agriculture and forest area still dominated the area in 2019, with the wide area around 56.6% and 25%, followed by dry land agriculture (9.5%), built-up area (3.7%), and paddy fields (Table 3). Water bodies, bare soil, and dry shrub have a wide area of less than 1%.

Land use and land cover changes

The result of an analysis of LULCC in the catchment area showed the degradation of LULC. This is indicated by the decreasing essential land use type, where forest area was found to be very important for ecohydrological services, while paddy fields are crucial for food safety and security. The decreasing forest area and paddy fields will threaten the environmental services of the area. Based on the result, the forest area decreased to approximately 132 ha/year, with a total conversion of 2,261 in 1993-2006 and 1,167 ha in 2006-2019. Meanwhile, the paddy fields were reduced by around 78 ha/year, with a total area conversion of 1,022 ha in 1993-2006, and 1,004 ha in 2006-2019. In contrast, the built-up area and dry land agriculture increase significantly. The built-up area increased by 54 ha/year, with a total increasing area of 594 ha in 1993-2006, and 817 ha in 2006-2019. The dry land agriculture increased by 141 ha/year, with a total area of 2,842 ha in 1993-2006, and 820 ha in 2006-2019. Mixed dry land agriculture increased by 214 ha in 1993-2006 and 533 ha in 2006-2019, with an average of 29 ha/year. The LULCC analysis in the catchment area is presented in Table 4. The increase in the area of water bodies is due to the establishment of the Musi Hydropower-Plant in 2006. The reservoir of Musi Hydropower-Plant resulted from inundation of the area of paddy fields, dry land agriculture, and mixed dry land agriculture around the Musi River which was fixed to be the reservoir area. Meanwhile, the bare soil and dry shrub tend to decrease with an average of 3 ha/year and 13 ha/year, respectively.

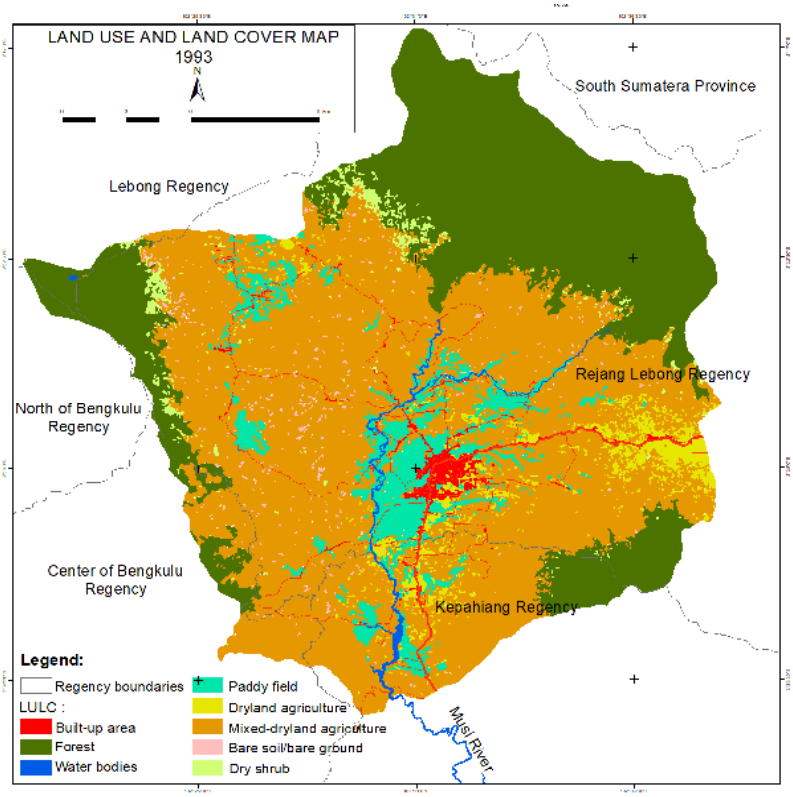

Figure 7. LULC map of 1993.

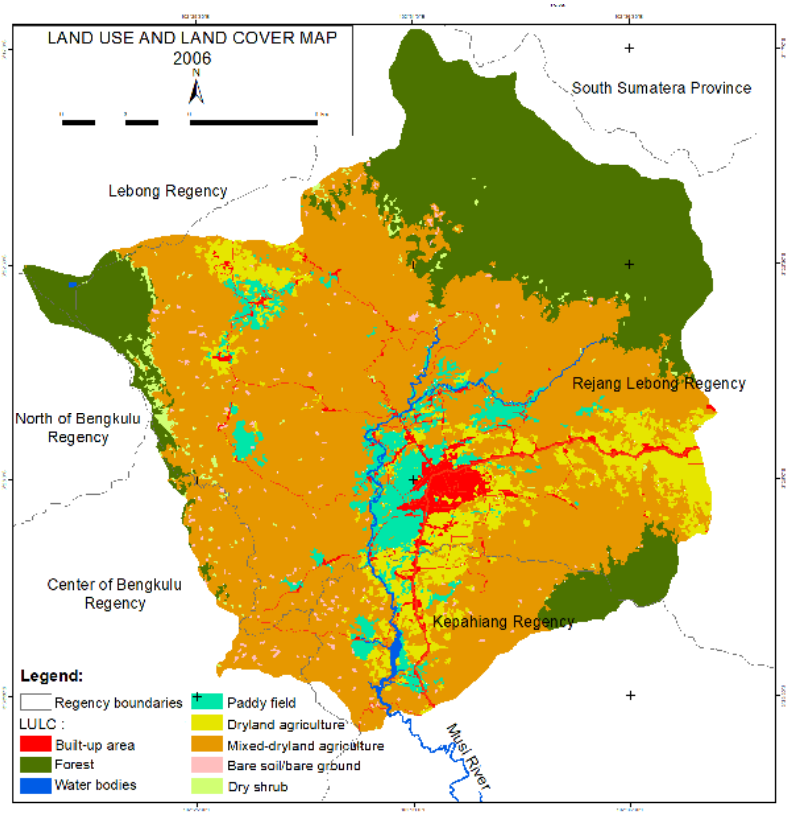

Figure 8. LULC map of 2006.

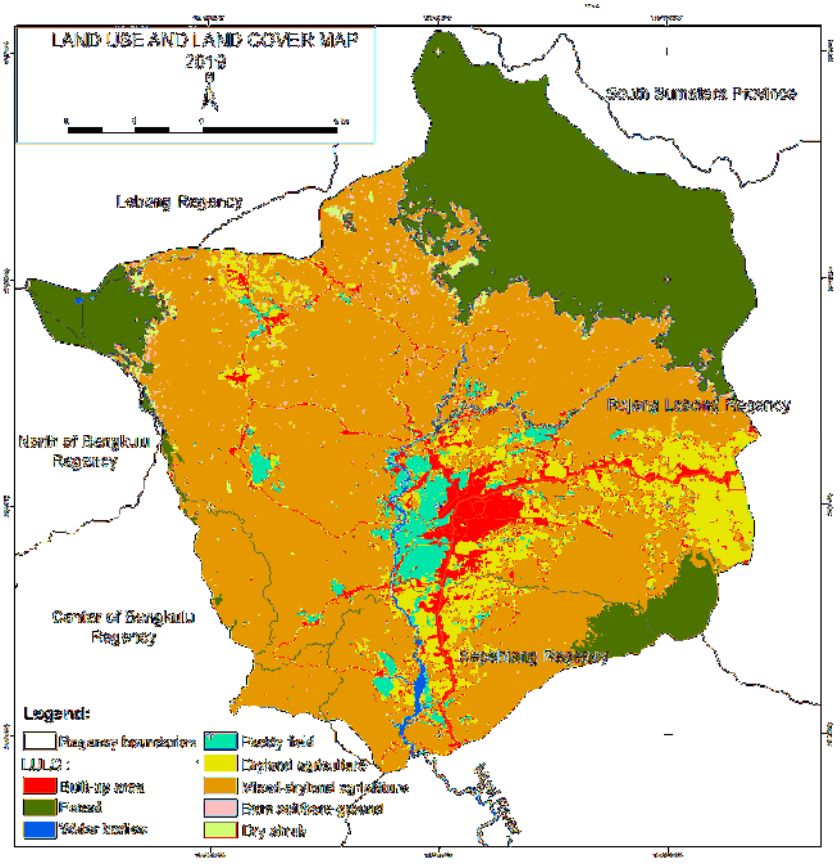

Figure 9. LULC map of 2019.

Table 3. LULC 1993-2019.

Land Use Type	1993		2006		2019	
	ha	%	ha	%	ha	%
Built-up area	818	1.3	1,412	2.3	2,229	3.7
Forest area	18,580	30.7	16,320	26.9	15,153	25.0
Water bodies	147	0.2	210	0.3	210	0.3
Paddy fields	4,044	6.7	3,023	5.0	2,019	3.3
Dry land agriculture	2,116	3.5	4,958	8.2	5,778	9.5
Mixed dry land agriculture	33,534	55.3	33,748	55.7	34,281	56.6
Bare soil/bare ground	487	0.8	383	0.6	403	0.7
Dry shrub	890	1.5	563	0.9	544	0.9
Total	60,616	100	60,616	100	60,616	100

Table 4. LULCC in the Musi Hydropower-Plant Catchment Area 1993-2019.

Land Use Type	1993-2006 (ha)	2006-2019 (ha)	1993-2019 (ha)	Annual Change (ha)
Built-up area	594	817	1.412	54
Forest area	-2,261	-1,167	-3,428	-132
Water bodies	63	-1	63	2
Paddy fields	-1,022	-1,004	-2,025	-78
Dry land agriculture	2,842	820	3.662	141
Mixed dry land agriculture	214	533	747	29
Bare soil/bare ground	-105	20	-84	-3
Dry shrub	-327	-19	-346	-13

Driving factors

The five potential driving factors of LULCC are elevation, slope, population density, and distance to roads, rivers, as well as settlements. The Cramer's V indicated that elevation, slope, population density, and distance to roads and settlements have significant correlations to land use and land cover change in the catchment area, shown by the Cramer's V of more than 0.15. The distance to rivers has Cramer's V less than 0.15 (Table 5).

Table 5. Spatial driver of LULCC.

Variables	Cramer's V	P Value
Elevation	0.3016	0.0000
Slope	0.2033	0.0000
Distance to roads	0.3105	0.0000
Distance to rivers	0.1249	0.0000
Distance to Settlements	0.3692	0.0000
Population density	0.4175	0.0000

The transition probability matrix

The prediction of LULC in 2032 based on the transition probability matrix resulted from CA-Marcov Chain analysis in LCM Module on IDRISI Terrset. The LULC of 1993 and 2006 was the input of the model, while LULC 2019 was the image reference of the validation model. According to the kappa coefficient of 0.8657 and agreement cells of 90.81%, the model was used to predict LULC in 2032. The transition probability matrix is shown in Tables 6 and 7. The transition probability matrix of prediction land use and land cover in 2019 shows that the built-up area and water bodies are settled and did not change to the other land use type. The forest area is changed to mixed dry land agriculture, bare soil, and dry shrub. Meanwhile, paddy fields tend to change to the built–up area, water bodies, dry land agriculture and mixed dry land agriculture. It was also discovered that mixed dry land agriculture could change to the built-up area, dry land agriculture, and bare land. The bare soil tends to convert to dry and mixed-dry land agriculture. The dry shrub tends to convert to bare land and dry and mixed-dry land agriculture.

Prediction accuracy

The predicted LULC in 2019 has a K standard of 0.87, with a total agreement of 90.81%. This indicates that the prediction of LULC is acceptable and reliable for predicting the next LULC in 2032. The comparison of LULC prediction in 2019 with the actual value showed that the overall predicted land use type is accurate by more than 80%. The highest accuracy is the built-up area and mixed-dry agricultural land, with a value of 99%, while dry agricultural land is the lowest, with 83%, as shown in Table 8.

Table 6. Transition probability matrix of prediction of LULC 2019

	BA	F	W	P	DA	MA	BS	S
BA	1.00	0.00	0.00	0.00	0.00	0.00	0.00	0.00
F	0.00	0.86	0.00	0.00	0.00	0.12	0.00	0.02
W	0.00	0.00	1.0	0.00	0.00	0.00	0.00	0.00
P	0.02	0.00	0.01	0.75	0.12	0.10	0.00	0.00
DA	0.10	0.00	0.00	0.00	0.70	0.20	0.00	0.00
MA	0.01	0.00	0.00	0.00	0.09	0.88	0.01	0.00
BS	0.00	0.00	0.00	0.00	0.03	0.95	0.02	0.00
S	0.00	0.00	0.00	0.00	0.02	0.70	0.02	0.16

BA = the built-up area, F = forest, W = water bodies, P = paddy fields, DA = dry land agriculture, MA = mixed dry land agriculture, BS = bare soil, S = shrub.

Table 7. Transition probability matrix of prediction of LULC 2032.

	BA	F	W	P	DA	MA	BS	DS
BA	1.00	0.00	0.00	0.00	0.00	0.00	0.00	0.00
F	0.00	0.75	0.00	0.00	0.01	0.22	0.00	0.02
W	0.00	0.00	1.00	0.00	0.00	0.00	0.00	0.00
P	0.05	0.00	0.00	0.57	0.18	0.19	0.00	0.00
DA	0.16	0.00	0.00	0.00	0.51	0.32	0.00	0.00
MA	0.03	0.01	0.00	0.00	0.14	0.81	0.01	0.00
BS	0.01	0.01	0.00	0.00	0.10	0.86	0.01	0.00
DS	0.01	0.11	0.00	0.00	0.08	0.76	0.01	0.03

BA = the built-up area, F = forest, W = water bodies, P = paddy fields, DA = dry land agriculture, MA = mixed dry land agriculture, BS = bare soil, S = shrub.

Table 8. The LULC 2019 and predicted LULC 2019.

Land Use Type	LULC 2019		Predicted LULC 2019		Prediction Accuracy (%)
	ha	%	ha	%	
Built-up area	2,229	3.7	2,249	3.7	99
Forest area	15,153	25.0	14,441	23.8	95
Water bodies	210	0.3	202	0.3	97
Paddy fields	2,019	3.3	2,283	3.8	87
Dry land agriculture	5,778	9.5	6,744	11.1	83
Mixed dry land agriculture	34,281	56.6	33,877	55.9	99
Bare soil/bare ground	403	0.7	364	0.6	90
Dry shrub	544	0.9	456	0.8	84
Total	60,616	100	60,616	100	

Predicted LULC in 2032

The predicted LULC in 2032 shows that mixed dry land agriculture still dominated the area, with a coverage of 56%. The forest area coverage is 21.3%, followed by dry land agriculture, the built-up area, dry shrub, bare soil, and water bodies, with coverage at 12.8%, 5.3%, 0.7%, 0.6%, and 0.3%, respectively. The predicted LULC in 2032 is presented in Figure 10.

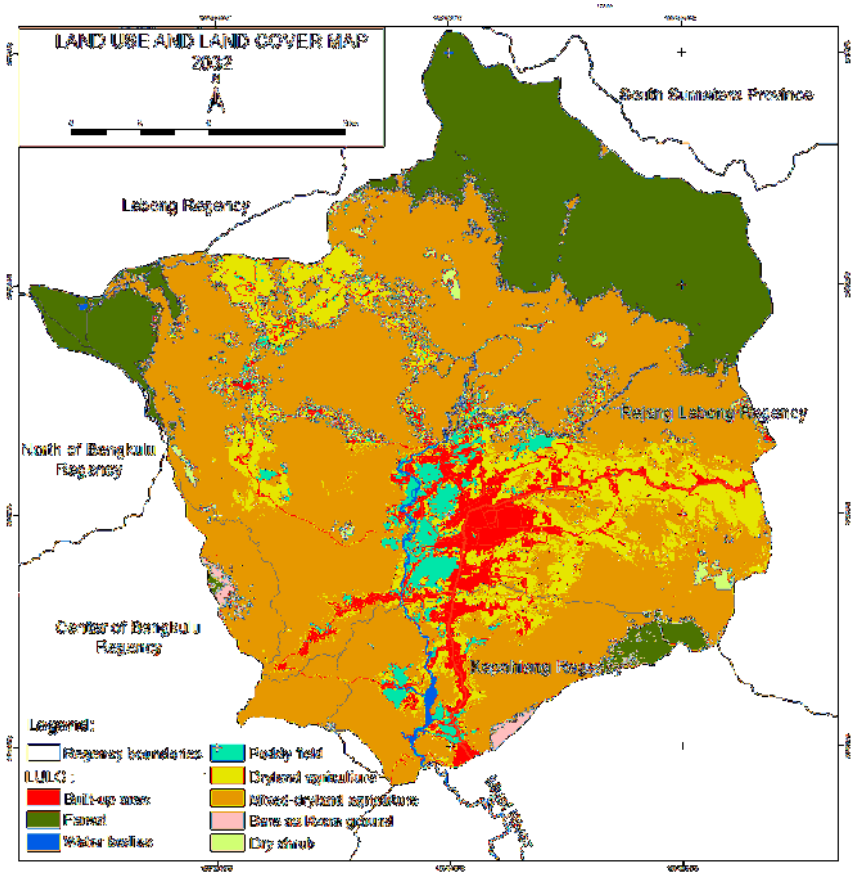

Figure 10. The projected LULC of 2032.

Soil erosion rate 1993-2019

The prediction of soil erosion rates shows that LULCC contributed to the increase in soil erosion rates, from 75 t/ha/year in 1993 to 93 t/ha/year in 2006 and 113 t/ha/year in 2019, which continues to increase until 122 t/ha/year in 2032, as shown in Figure 11. The prediction of soil erosion in 1993 varied from 0-46,943 t/ha/year, with an average of 75 t/ha/year. Based on the severity class of soil erosion, most of the area has a very light soil erosion class, followed by heavy, very heavy, medium, and light, with values of 86.7%, 4.4%, 4.1%, 3.6%, and 1.2%. In 2006, the soil erosion rates varied from 0-31,947 t/ha/year, with an

average of 93 t/ha/year. The area was dominated by very light, followed by the heavy class, very heavy, medium, and light, with values of 85.7%, 4.9%, 4.8%, 3.3%, and 1.2%. The soil erosion in 2019 varied from 0-20,538 t/ha/year, with an average of 113 t/ha/year. The dominant class was the very light, followed by the very heavy class, heavy class, medium, and light, with the proportion of 84.9%, 5.9%, 4.8%, 3.1%, and 1.4%. The soil erosion maps of 1993, 2006, and 2019 are presented in Figures 12, 13, and 14, while the every class is in Table 9. The soil erosion class showed that the very heavy class tends to increase from 4.1% to 4.8% and 5.9%, while the very light classes decreased from 86.7% to 85.7%, and 84.9% in 1993, 2006, and 2019. These phenomena indicate that LULCC contributes to the change in soil erosion rates.

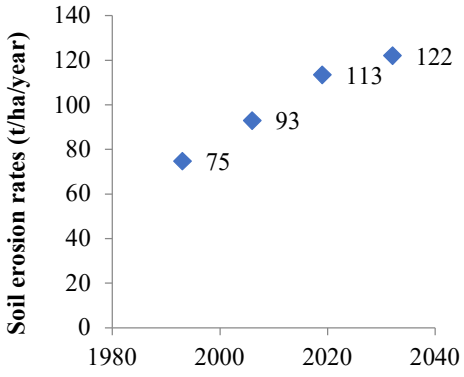

Figure 11. The average soil erosion rates.

Table 9. Percentage area of soil erosion class 1993-2019.

Soil erosion class	Soil erosion rates (t/ha/year)	Area (%)		
		1993	2006	2019
Very light	0-15	86.7	85.7	84.9
Light	15-60	1.2	1.2	1.4
Medium	60-180	3.6	3.3	3.1
Heavy	180-480	4.4	4.9	4.8
Very heavy	>480	4.1	4.8	5.9
Total		100	100	100
Average (t/ha/year)		75	93	113

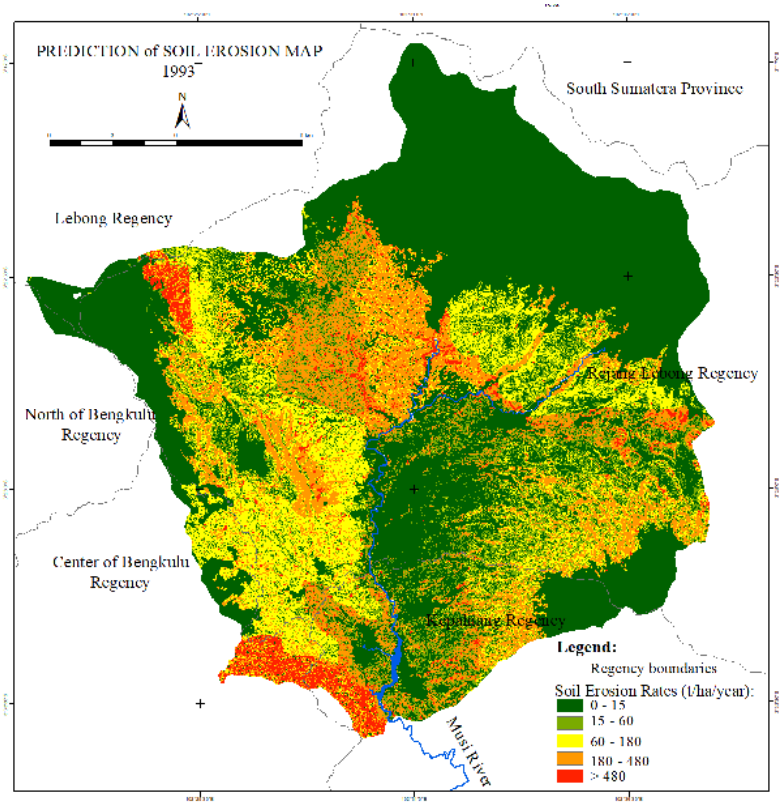

Figure 12. Erosion map 1993.

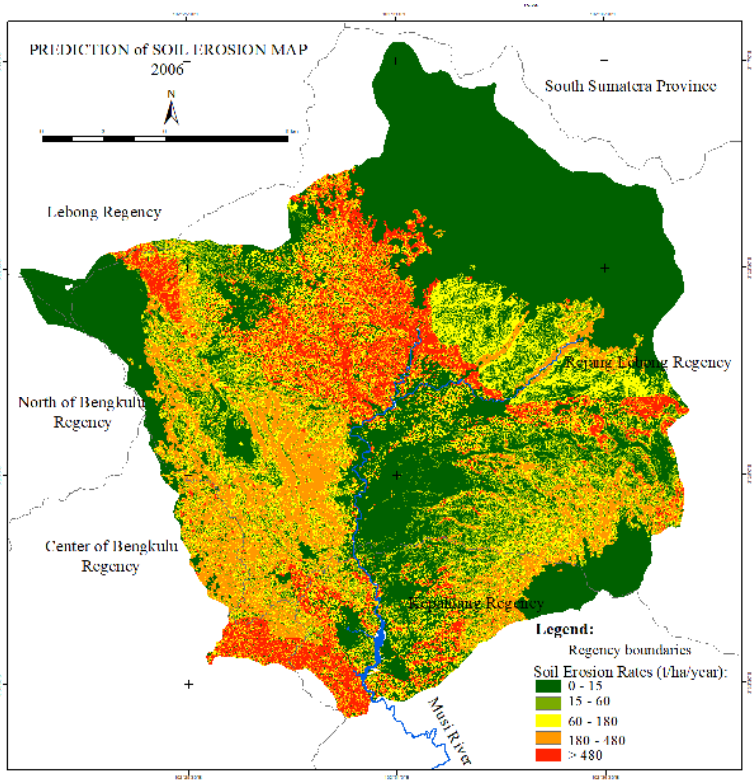

Figure 13. Erosion map 2006

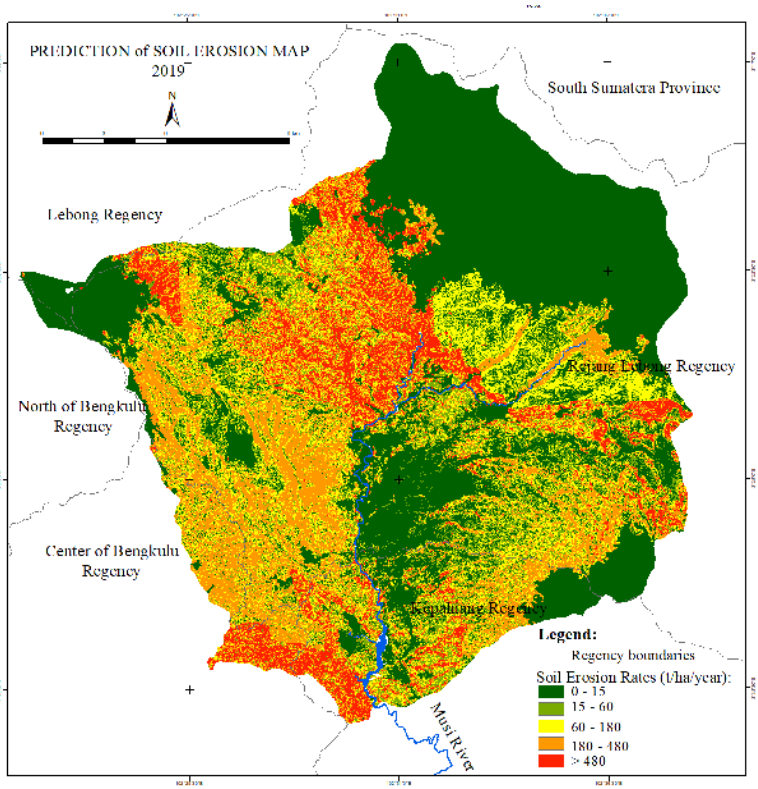

Figure 14. Erosion map 2019.

Soil erosion rates in 2032

As LULCC continues to increase, the prediction of soil erosion rates in 2032 showed an average of soil 122 t/ha/year, which will vary from 0-21,437 t/ha/year. The results showed that the dominant class was very light, followed by very heavy, heavy, medium, and light at 84.3%, 6.3%, 4.6%, 3.2%, and 1.6%, respectively. Increasing soil erosion rates will contribute to the high sedimentation in the reservoir and interfere with the hydropower plant operation. The classification of the soil erosion severity class of 2032 is presented in Table 10 and Figure 15.

Table 10. The predicted soil erosion class of 2032.

Soil erosion class	Soil erosion rates (t/ha/year)	Area (%)	
		ha	%
Very light	0-15	51,096	84.3
Light	15-60	967	1.6
Medium	60-180	1,964	3.2
Heavy	180-480	2,775	4.6
Very heavy	>480	3,814	6.3
Total Area (ha)		60,616	100
Average (t/ha/year)		113	122

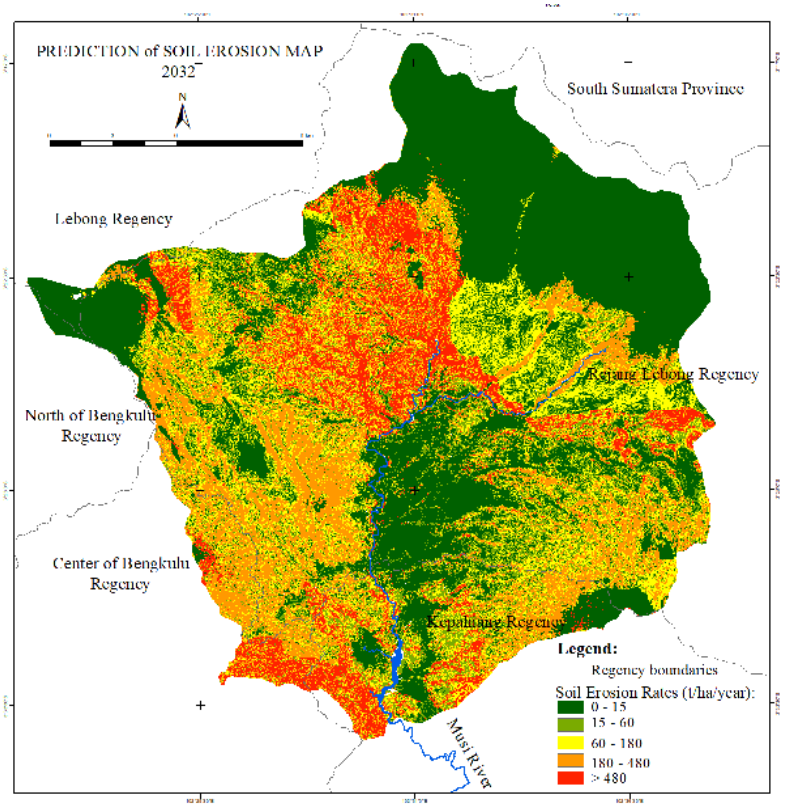

Figure 15. The soil erosion severity map of 2032.

Predicted sediment yield

The prediction of sediment yield shows the increasing soil erosion rates followed by sediment yield. In 1993, the sediment yield was 68,048 t/ha/year. The sediment yield increased to 84,533 t/ha/year in 2006, and 103,190 t/ha/year in 2019 and is predicted to reach 111,028 t/year in 2032. Generally, sediment yield is the amount of sediment that reaches the water bodies, as a function of the Sediment Delivery Ratio (0.015). The sediment will interfere with the operation of the power Plant by reducing the supply of water to the generator. The predicted sediment yields are presented in Figure 16.

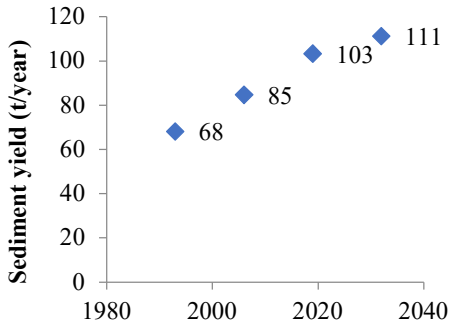

Figure 16. The predicted sediment yields.

Discussion

The sustainability of the Musi Hydropower-Plant catchment area is affected by the condition of LULC. Therefore, the analysis was performed to show the dynamics of LULC in the catchment area. The result showed that in 1993, mixed dryland agriculture and forest cover dominated with 55.5% and 30.7%, respectively. It is followed by paddy fields, dry land agriculture, shrubs, bare soil, and water body with percentages are 6.7%, 3.5%, 1.5%, 1.3%, 0.8%, and 0.2%, respectively. In 2019, mixed dryland agriculture and forest cover still dominated the area. The mixed-dryland agriculture slightly increased to 56.6%, while the forest cover significantly decreased to 25.0%. The paddy fields also decrease to 3.3%, while built-up area and dryland agriculture enlarge to 3.7% and 9.5%, respectively. Increasing mixed dryland agriculture, dryland agriculture, and built-up area and then decreasing forest cover and paddy fields indicate the high human activities in the catchment area. Hu et al. (2021) stated that changes in LULC are increasingly affecting the land properties and the provision of ecosystem services. The decreasing forest area indicated that the Musi Hydropower-Plant catchment area is susceptible to degradation.

Forest cover is very crucial in controlling eco-hydrological processes. Based on the transition probability matrix, forest cover tends to convert to dry and mixed-dryland agriculture, bare soil, and shrubs. It means that deforestation is closely related to agricultural activity. Decreasing forest area implies increasing cultivated land. There is no plantation such as palm oil or rubber plantation. Forest area converted to small-scale agriculture with an average value of 1-2 ha for each farmer. Austin et al. (2019) reported that small-scale agriculture and small-scale plantation contributed to the national scale deforestation in Indonesia from 2001 to 2016, with the value of 15% and 7%, respectively. It means that deforestation in the catchment area also contributed to the national scale of deforestation. The forest area is predicted to decrease in 2032, with a value of 21.7%.

Deforestation in the Musi Hydropower-plant catchment area emerges as a crucial issue because of its impact on the environmental problem. Deforestation in this area is closely related to the shifting cultivation culture. With the limited land availability, people tend to penetrate the primary forest area. Coincident to Susanto et al. (2018), the asymmetric deforestation concept is also the main driving factor of deforestation in this area. Some people claim that forest is a common pool resource and disagree with the borderline of protected forest area stated by the government. Disagreement about the borderline of protected forest areas implies the rate of deforestation.

Paddy fields decreased significantly from 6.7% in 1993 to 3.3% in 2019. Paddy fields convert to the built-up area, bare soil, and dry and mixed-dryland agriculture. Decreasing paddy fields threaten food safety and security. Permanently conversion of paddy fields to the built-up area as the impact of urbanization reduces land productivity. Urbanization will convert strategic fields, especially paddy fields (Rustiadi et al., 2020). Paddy fields predicted still decrease to 2.9% in 2032.

In the other site, decreasing forest cover and paddy fields implies increasing the built-up area and dry and mixed-dryland agriculture. The built-up area and dryland agriculture are predicted to increase in 2032, while mixed dryland agriculture will slightly decrease in 2032. Increasing the built-up area is the implication of increasing population. People need a place to stay and also need materials for their activities. Land use and land cover change are a consequence of the competition for land use.

LULCC is proceeded by the influence of various aspects. Based on Cramer's Value, population density is the driving factor that significantly influences the LULCC, with a value of 0.4175. The increasing population is followed by increasing demand for land, indicated by the high growth of the built-up area, from 818 ha in 1993 to 2,229 ha in 2019. The next factor is the distance to settlements, with a value of 0.3692, followed by distance to roads, elevation, and slope, with a value of 0.3105, 0.3016, and 0.2033, respectively. Distance to settlements and roads is related to the accessibility of objects to change, while elevation and slope are related to the suitability of land use change. Elevation, slope, distance to roads, distance to settlements, and population density are the factors suggested as driving factors of LULC (Allan et al., 2022).

The phenomenon of LULCC in the catchment area can be used as a baseline for the decision maker to make better land use planning. LULCC is known to have positive and negative impacts. Based on the predicted map, the positive outcomes can be optimized, while the detrimental impact can be reduced. Decreasing forest area and paddy fields in 2032 is good information for decision-makers. Deforestation lessens by implementing the regulation of the protected area, payment of environmental services, developing a community-based forest, and other programs that support the sustainability of forest areas and improve human well-being (Novick et al., 2022). Meanwhile, decreasing paddy fields should be avoided with the implementation of the regulation of Sustainable Food Agriculture Land ("LP2B-Lahan Pangan Pertanian Berkelanjutan").

LULCC in the catchment area contributed to the increasing soil erosion and sedimentation rates. The soil erosion rate in 1993 was 75 t/ha/year, which increased to 93 t/ha/year in 2006 and 113 t/ha/year in 2019. The soil erosion rates are predicted to continue to increase in 2032 with a value of 122 t/ha/year. Because of the limited data, the soil erosion factor assumed that soil erodibility (K) and slope-length steepness (LS) are constant, while rainfall erosivity (R)

and cover management (C) and land management or support practice (P) are different. The rainfall erosivity index showed an increasing value from 1,795 MJmm/ha/year in 1993 to 1,956 MJmm/ha/year in 2006 and 2,283 MJmm/ha/year in 2019. Meanwhile, the C factor and P factor are different each year, derived from LULC. Increasing the built-up area, dry and mixed-dryland agriculture implies the increasing value of the C factor. It means that LULCC in the catchment area contributed to the increasing soil erosion rates. This phenomenon is similar to the contribution of global agricultural activities on the increasing total soil erosion and soil erosion rates in the tropical region was 3.2 Gt and 0.22 Mg/ha/year (Hu et al., 2021), the impact of LULC dynamic on soil erosion and sedimentation in Ethiopia (Kidane et al., 2019), and effect of LULC on soil erosion rates in Southern Spain (Millazo et al., 2022). As same as with the contribution of LULCC on soil erosion rates, the sediment yields increased from 68,048 t/year in 1993 to 84,533 t/year in 2006 and 103,190 t/year in 2019.

Soil erosion and sedimentation are predicted to continue to increase in 2032, with a value of 122 t/ha/year and 111,028 t/year, respectively. The soil erosion factors in this prediction assumed constant except for C and P factors. It means that this prediction purely showed the contribution of LULC. The predicted value of soil erosion and sedimentation in 2032 is considered an instrument for managing the environment, especially in the context of integrating the outcomes of environmental effects and human well-being (Novick et al., 2022). The data and information about land use and land cover changes in the Musi Hydropower-Plant Catchment area and their impact on soil erosion and sedimentation are useful for decision-makers and policymakers to make better management planning.

Conclusion

The Musi Hydropower-Plant catchment area is vulnerable to degradation, as shown by the decreasing forest cover and paddy fields. The forest cover decreased from 18,580 ha in 1993 to 15,153 ha in 2019. At the same period, paddy fields decreased from 4,044 ha to 2,019 ha. The forest area and paddy fields are predicted to continue to decrease, becoming 12,907 ha and 1,729 ha in 2032. In contrast, the built-up area and dry land agriculture increased significantly, from 818 ha and 2,116 ha in 1993 to 2,229 ha and 5,778 ha in 2019, respectively. The increase of built-up area and dry land agriculture will continue to increase and reach 3,240 ha and 7,774 ha in 2032. The LULCC contributed to the increase of soil erosion rates from 75 t/ha/year in 1993 to 93 t/ha/year in 2006, and 113 t/ha/year in 2019. The soil erosion rates fixed continued to increase in 2032 becoming 122 t/ha/year. Increasing soil erosion rates contributed to the increasing sediment yield, from 68,048 t/year in 1993 to 84,533 t/year in 2006, and 103,190 t/year in 2019. The sediment yield continued to increase in 2032, becoming 111,028 t/year.

Acknowledgements

The authors are grateful to The Ministry of Education, Culture, Research, and Technology for the scholarship of BPPDN DIKTI 2017, The Faculty of Agriculture University of Bengkulu, The Musi Hydropower-Plant, and The Meteorological, Climatological, and Geophysical Agency of Pulau Baai Bengkulu, Indonesia for the supporting data for this research.

References

Allan, A., Soltani, A., Abdi, M.H., and Zarei, M. 2022. Driving forces behind land use and land cover change: A systematic and bibliometric review. *Land* 2022,11:1222, doi:10.3390/land11081222.

Amri, K., Halim, A., Ngudiantoro, and Barchia M.B. 2014. Rainfall analysis for estimation of peak discharge and soil erosion on the catchment area of Musi Hydropower-Plant, Bengkulu, Indonesia. *2014 International Conference on Intelligent Agriculture. IPCBEE.*

Atulley, J.A., Kwaku, A.A., Gyamfi, C., Owushu-ansah, E.D.J., Adonadaga, M.A. and Nii, O.S. 2022. Reservoir sedimentation and spatiotemporal land use changes in their watersheds: the case of two sub-catchments of the White Volta Basin. *Environmental Monitoring and Assessment* 194:809, doi:10.1007/s10661-022-10431-y.

Austin, K.G., Schwantes, A., Yaofeng, Gu. and Kasibhatla, P.S. 2019. What causes deforestation in Indonesia? *Environmental Research Leters* 14:024007, doi:10.1088/1748-9326/aaf6db.

Borrellli, P., Allewel, C., Alvares P., Annace, J.A.A., Baartman, J., Ballabio, C., Bezak, N., Biddocu, M., Cerda. A., Chalisa, D., Chen, S., Chen, W., De Girolamo, A.M., Gessesse, G.D., Deumlich, D. and Dodato, N. 2021. Soil Erosion Modelling: A global review and statistical analysis. *Science of the Total Environment* 780: 146494, doi:10.1016/j.scitotenv.2021.146494.

Briassoulis, H. 2020. *Analysis of Land Use Change: Theoretical and Modeling Approaches.* WVU Research Repository, Virginia, US.

Chaves, M.E.D., Picoli, M.C.A. and Sanches, I.D. 2020. Recent Application of Landsat 8/OLI and Sentinel-2/MSI for land use and land cover mapping: a systematic review. *Remote Sensing* 12:3062, doi:10.3390/rs12183062.

Comber, A., Fisher, P. and Wardsworth, R. 2015. Text Mining Analysis of Land Cover Semantic Overlap. (eds), *Land Use and Land Cover Semantics. Principles, Best Practices, and Prospects*. CRC Press, Taylor and Francis Group. Boca Raton, London, New York. pp.192-207.

Dangulla, M., Munaf, L.A. and Mohammad, F.R. 2020. Spatio-temporal analysis of land use/land cover dynamics in Sokoto Metropolis using multi-temporal satellite data and Land Change Modeler. *Indonesian Journal of Geography* 52(3):306-316.

Ejegu, M.A. and Yegizaw, E.S. 2021. Modeling soil erosion susceptibility and LULC dynamics for land degradation management using geoinformation technology in Debre Tabor District, Northwestern highlands of Ethiopia.

Journal of Degraded and Mining Lands Management 9(2):2623-2633, doi:10.15243/jdmlm.2021.082.2623.

Endalew, T. and Biru, D. 2022. Soil erosion risk and sediment yield assessment with revised universal soil loss equation and GIS: The case of Nesha Watershed, Southwestern Ethiopia. *Results in Geophysical Sciences* 12:100049, doi:10.1016/j.ringps.2022.100049.

Foody, M.G. 2020. Explaining the unsuitability of the kappa coefficient in the assessment and comparison of the accuracy of thematic maps obtained by image classification. *Remote sensing of environment* 239: 111630, doi:10.1016/j.rse.2019.111630.

Gwapedza, D., Hughes, D.A., Slaughter, A.R. and Mantel, S.K. 2021. Temporal influences of vegetation cover (C) dynamism on MUSLE sediment yield estimation. NDVI Evaluation. *Water* 13:2707, doi:10.3390/w13192707.

Hu, X., Naess, J.S., Iordan, C.M., Bo Huang, Zhao, W. and Cherubini, F. 2021. Recent global land cover dynamics and implications for soil erosion and carbon losses from deforestation. *Anthropocene* 34:100291, doi:10.1016/j.ancene.2021.100291.

Jothimani, M., Getahun, E. and Abebe, A. 2022. Remote sensing, GIS, and RUSLE in soil loss estimation in Kuflo river catchment, Rift Valley, Southern Ethiopia. *Journal of Degraded and Mining Lands Management* 9(2):3307-3315, doi:10.15243/jdmlm.2022.092.3307.

Kidane, M., Bezie, A., Kesete, N. and Tolesa, T. 2019. The impact of land use and land cover change (LULCC) dynamics on soil erosion and sediment yield in Ethiopia. *Heliyon* 5:e02981, doi:10.1016/j.heliyon.2019.e02981.

Kokla, M., Baglatzi, and Kavouraz, A.M. 2015. Eliciting and Formalizing the Intricate Semantics of Land Use and land Cover Class Definitions. In: Ahlqvist, O., Varanka, D., Fritz, S. and Janowics, K. (eds), *Land Use and Land Cover Semantics. Principles, Best Practices, and Prospects*. CRC Press, Taylor and Francis Group. Boca Raton, London, New York. pp.86-103.

Kulimushi, L.C, Maniragaba, A., Choudhari, P., Elbeltagi, A., Uwemeye, J., Rushema, E. and Singh, S.K. 2021. Evaluation of soil erosion and sediment yield spatio-temporal pattern during 1990-2019, *Geomatics, Natural Hazards and Risk* 12(1):2676-2707, doi:10.1080/19475705.2021.1973118.

Ma, L., Li, M., Ma, X., Cheng, L., Du, P. and Liu, J. 2017. A review of supervised object-based land-cover image classification. *ISPRS Journal of Photogrammetry and Remote Sensing* 130:277-293, doi:10.1016/j.isprsjprs.2017.06.001.

Millazo, F., Fernandez, P., Pena, A. and Vanwalleghem, T. 2022. The resilience of soil erosion rates under historical land use change in agroecosystems of Southern Spain. *Science of the Total Environment* 822:153672, doi:10.1016/j.scitotenv.2022.153672.

Muddarisna, N., Yuniwati, E.D., Masruroh, H. and Oktaviansyah, A.R. 2021. The effectiveness of cover crops on soil loss control in Gede catchment of Malang Regency, Indonesia. *Journal of Degraded and Mining Lands Management* 8(2):2673-2679. doi:10.15243/jdmlm.2021.082.2673.

Mujiyo, Hardian, T., Widijanto, H. and Herawati, A. 2021. Effect of land use on soil degradation in Giriwoyo, Wonogiri, Indonesia. *Journal of Degraded and Mining Lands Management* 9(1):3063-3072, doi:10.15243/jdmlm.2021.091.3063.

Novick, B., Crouch, J., Ahmad, A., Rodiansyah, Muflihati, Kartikawati, S.M., Sudaryanti, Sagita, N. and Miller, A.E. 2022. Understanding interactions between human well-being and environmental outcomes through a community-led integrated landscape initiative in Indonesia. *Environmental Development* 45(2023):100791.

Obiahu, E.H. and Elias, E. 2020. Effect of land use land cover changes on the rate of soil erosion in the Upper Eyiohia river catchment of Afikpo North Area, Nigeria. *Environmental Chalanges* 1:100002, doi:10.1016/j.envc.2020.100002.

Pandey, S., Kumar, P., Zlatic, M., Nautiyal, R. and Panwar, V.P. 2021. Recent advance in assessment of soil erosion vulnerability in a watershed. *International Soil and Water Conservation Research* 9:305-318. doi:10.1016/j.iswcr.2021.03.001.

Patro, E.R., De Michele, C., Granata, G. and Biagini, C. 2022. Assessment of current reservoir sedimentation rate and storage capacity loss: an Italian overview. *Journal of Environmental Management* 320: 115826, doi:10.1016/j.jenvman.2022.115826.

Rustiadi, E., Pravitasari, A.E., Setiawan, Y., Mulya, S.P., Pribadi, D.O. and Tsutsumida, N. 2021. Impact of continuous Jakarta megacity urban expansion on the Jakarta-Bandung conurbation over the rice farm regions. *Cities* 111:103000, doi:10.1016/j.cities.2020.103000.

Sukisno, Widiatmaka, Purwanto, M.Y.J., Noorachmat, B.P. and Munibah, K. 2021. A review of land use land cover change in the catchment area of Musi Hydropower Plant in Bengkulu Province. *E3S Web of Conferences* 305:04001, doi:10.1051/e3sconf/202130504001.

Susanto, E., Lestari, N., Hapsari, M. and Krisdiyatmiko. 2018. Driving factors of deforestation in Indonesia: A case of Central Kalimantan. *Jurnal Studi Pemerintahan* 9(4):511-533.

Wang, Q., Xu, Y., Xu, Y., Wu, L., Wang, Y. and Han, L. 2018. Spatial hydrological responses to land use and land cover changes in a typical catchment of the Yangtze River Delta region. *Catena* 170: 305-315, doi:10.1016/j.catena.2018.06.022.

Yan, R., Zhang, X., Yan, S. and Chen, H. 2018. Estimating soil erosion response to land use/cover change in a catchment of the Loss Plateau, China. *International Soil and Water Conservation Research* 6:13-22, doi:10.1016/j.iswcr.2017.12.002.